Optical backscattering is correlated with phytoplankton carbon across the Atlantic Ocean

V. Martinez-Vicente,[1] G. Dall'Olmo,[1] G. Tarran,[1] E. Boss,[2] and S. Sathyendranath[1]

Received 27 November 2012; revised 7 February 2013; accepted 11 February 2013.

[1] Phytoplankton are an important component of the oceanic carbon cycle. Yet, due to methodological constraints, the carbon biomass of phytoplankton is poorly characterized. To address this limitation, we have explored the bio-optical relationship between *in situ* measurements of the particle backscattering coefficient at 470 nm, $b_{bp}(470)$, and the phytoplankton carbon concentration for cells with diameter less than 20 μm (C_f). We found a significant relationship between $b_{bp}(470)$ and C_f for Atlantic oceanic waters with chlorophyll-a concentrations less than 0.4 mg m^{-3} (or $b_{bp}(470) < 0.003\ m^{-1}$). This relationship could be used to estimate C_f from data collected by *in situ* autonomous platforms and from remote sensing of ocean color. **Citation:** Martinez-Vicente, V., G. Dall'Olmo, G. Tarran, E. Boss, and S. Sathyendranath (2013), Optical backscattering is correlated with phytoplankton carbon across the Atlantic Ocean, *Geophys. Res. Lett.*, *40*, doi:10.1002/grl.50252.

1. Introduction

[2] Phytoplankton are fundamental drivers of the ocean carbon cycle and they sustain the oceanic ecosystems. Yet, direct measurements of phytoplankton carbon remain scarce due to the lack of reliable methods. The most direct method for quantifying phytoplankton carbon *in situ* relies on cell counts and bio-volume conversion into carbon biomass using empirical relationships [*Strathmann*, 1967]. Microscopy is used to enumerate the larger phytoplankton cells (i.e., diameter greater than 20 μm [*Holligan et al.*, 1984]), whereas flow cytometry is used to count smaller cells (i.e., *Prochlorochoccus* spp., *Synecoccocus* spp. and eukaryotes) [*Zubkov et al.*, 1998; *DuRand et al.*, 2001; *Tarran et al.*, 2001; *Tarran et al.*, 2006]. Transmission electron microscopy and X-ray microanalysis have also been employed to quantify phytoplankton biomass [*Heldal et al.*, 2003].

[3] An alternative approach to the collection and analysis of water samples is to use the optical backscattering coefficient of particles (b_{bp}) as a proxy for phytoplankton carbon [*Behrenfeld et al.*, 2005]. Particulate backscattering is an inherent optical property retrievable at a global scale from ocean color remote sensing [*Lee et al.*, 2002] or directly measured from *in situ* autonomous platforms [*Boss et al.*, 2008]. However, evaluation of this approach has not yet been attempted. The objective of this study is to explore the empirical relationship between b_{bp} and phytoplankton carbon using *in situ* data.

2. Methods

[4] Samples were collected during the 19th Atlantic Meridional Transect cruise (hereafter AMT19) from 48°N to 41.5°S (13 October to 1 December 2009, Figure 1A). Profiles of particulate optical backscattering at 470 nm, $b_{bp}(470)$, and flow-cytometric phytoplankton cell abundances were measured along the transect following established protocols (Supplementary material: Methods). Surface underway measurements of $b_{bp}(470)$, total chlorophyll-a (TChl-a), and particulate organic carbon (POC) were also determined (Supplementary material: Methods) [*Van Heukelem and Thomas*, 2001; *Behrenfeld and Boss*, 2006; *Dall'Olmo et al.*, 2009; *Dall'Olmo et al.*, 2012].

[5] The relative differences between $b_{bp}(470)$ measurements from the optical package casts and continuous underway system were quantified by the percent residuals $\left(R = 100 \times \left(b_{bp}^{underway}/b_{bp}^{opt.\ cast} - 1\right)\right)$. The bias was −16% (i.e., median of R), and the precision was 7% (i.e., half the central 68th percentile of R, N = 24).

[6] Data were selected from surface to $1.5Z_{eu}$ where Z_{eu} is the (1%) euphotic depth [*Claustre et al.*, 2008]. We will also refer to the first optical depth, approximated by $Z_{eu}/4.6$ following *Gordon and McCluney* [1975].

[7] The following phytoplankton groups were counted by flow cytometry in this study: *Prochlorococcus* spp., *Synechococcus* spp., picoeukaryotic phytoplankton, cryptophytes, coccolithophores, and other nanophytoplankton. Heterotrophic bacteria were not included. The phytoplankton carbon concentration (in mgC m^{-3}) from flow cytometry (f) for each phytoplankton group (i) and each sample (j), $C_f(i,j)$, was calculated as:

$$C_f(i,j) = N(i,j)\varepsilon(i)V(i) \quad (1)$$

where $N(i,j)$ are phytoplankton abundances (cell m^{-3}); $\varepsilon(i)$ is cellular carbon per unit of volume (fgC μm^{-3}) and $V(i)$ is the mean cell volume (μm^3). The total phytoplankton carbon concentration per sample j, i.e., $C_f(j)$ was the sum of the contributions from each phytoplankton type. A Monte Carlo method was employed to estimate the uncertainty in C_f (i.e., δC_f) as well as its major sources of error (Supplementary material: Methods).

[8] To describe the relationship between C_f and $b_{bp}(470)$ within $1.5Z_{eu}$, we used a Type II linear regression, assigning a value of uncertainty to each point. Model performance was

All Supporting Information may be found in the online version of this article.

[1]Plymouth Marine Laboratory, Plymouth, UK.
[2]School of Marine Sciences, University of Maine, Orono, Maine, USA.

Corresponding author: V. Martinez-Vicente, Plymouth Marine Laboratory, Propect Place, The Hoe, PL1 3DH, Plymouth, UK (vmv@pml.ac.uk)

0094-8276/13/10.1002/grl.50252

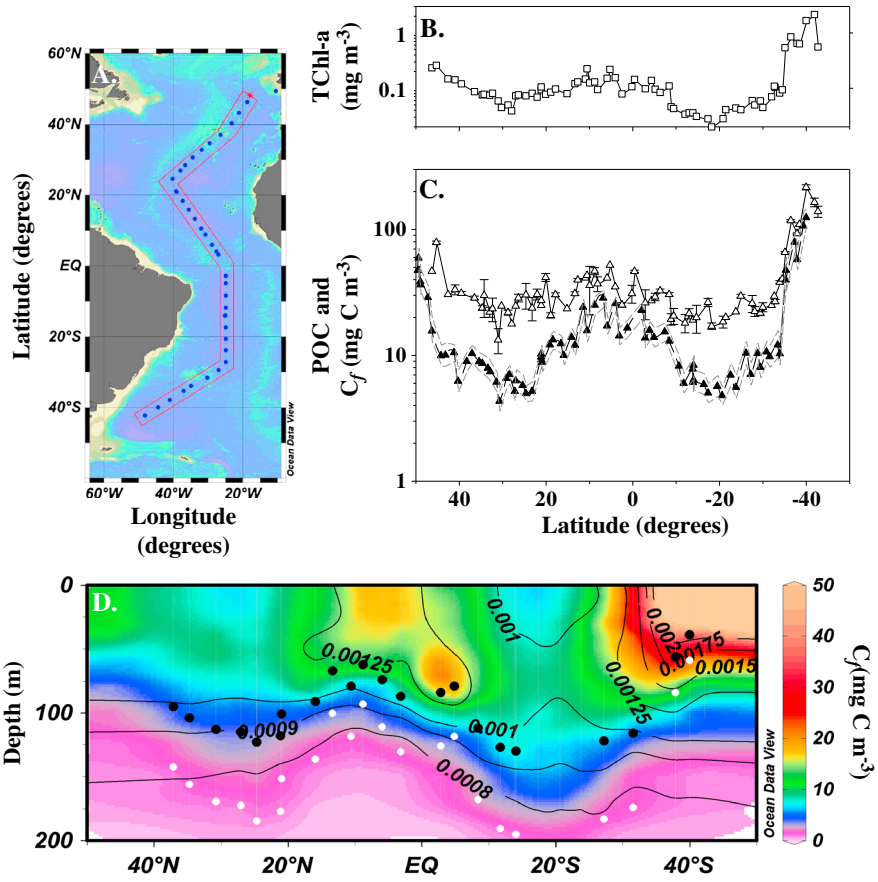

Figure 1. (A) Map of stations occupied during the AMT19 cruise. (B) Surface chlorophyll (TChl-a). (C) Surface particulate organic carbon concentration (POC, empty triangles, mean ± SD, N = 3 replicates) and phytoplankton carbon from flow cytometry at depths less than 10 m (C_f, filled triangles, median from Monte Carlo realizations; grey dashed lines are 16th and 84th percentiles). (D) Vertical section of C_f (color scale) and particle backscattering coefficient (b_{bp}(470), contour lines). Position of euphotic depth (Z_{eu}, black dots) and 1.5Z_{eu} (white dots).

evaluated in terms of the root mean square deviation (RMSD, [*Gauch et al.*, 2003; *Pineiro et al.*, 2008], $RMSD = \left(1/(N-1)\sum_{i=1}^{N}\left(C_m(j) - C_f(j)\right)\right)^{0.5}$), where C_m is the modelled phytoplankton carbon. Bias was described by the median of relative (signed) residuals between C_m and C_f, and precision by half the central 68th percentile of the relative residuals between C_m and C_f.

Table 1. Diameters (D, in μm) and Intra-cellular Carbon Concentrations (ε, in fgC μm^{-3}) Means and Standard Error (SE) Used to Compute C_f

	D	Reference	ε	Reference
Prochlorococcus spp.	0.68 ± 0.03 N = 3	*Heldal et al.* [2003]	214 ± 28 N = 3	*Heldal et al.* [2003]
Synechococcus spp.	1.22 ± 0.06 N = 6	*Heldal et al.* [2003]	203 ± 24 N = 6	*Heldal et al.* [2003]
Picoeukaryotes	1.56 ± 0.01[c] N = 3 3.13[a] ± 0.80[c] N = 3	*Tarran et al.* [2006]	220 ± 11[d] N = 37	*Booth* [1988] *Mullin et al.* [1966]
Nanoeukaryotes	4.30[b] ± 0.80[c] N = 3	*Tarran et al.* [2006]	220 ± 11[d] N = 37	*Booth* [1988] *Mullin et al.* [1966]
Cryptophytes	5.90 ± 0.94[c] N = 3	*Tarran et al.* [2006]	220 ± 11[d] N = 37	*Booth* [1988] *Mullin et al.* [1966]
Coccolithophorids	6.07 ± 0.51[c] N = 3	*Tarran et al.* [2006]	285 ± 25 N = 3	*Saunders* [1991] as cited in *Tarran et al.* [2006]

[a]Diameter for oligotrophic and eutrophic areas.
[b]Diameter for temperate areas.
[c]SE obtained from size fractionation experiments on board AMT-13, unpublished data, G.Tarran.
[d]SE obtained from all the data points in *Mullin et al.* [1966].

3. Results

[9] Surface TChl-a, POC, and C_f varied across the Atlantic Ocean following similar patterns. Lower TChl-a, POC, and C_f were found in the gyres, while greater values were found in the temperate and equatorial provinces (Figures 1B and 1C). The latitudinal variations of $b_{bp}(470)$ were consistent with previous studies in the Atlantic Ocean [*Stramski et al*., 2008; *Balch et al*., 2010] (Figure 1D). Similarly, the spatial variations in TChl-a and POC were consistent with observations from previous AMT cruises [*Perez et al*., 2006; *Poulton et al*., 2006a, 2006b; *Balch et al*., 2010]. C_f was higher than in previous studies in this area at different times of the year, but its latitudinal patterns were qualitatively consistent with studies using the same methodology [*Zubkov et al*., 2000; *Tarran et al*., 2006]. Furthermore, our C_f values fell within the range determined by other approaches [*Maranon et al*., 2000; *Perez et al*., 2006] and were lower than concurrent measurements of POC (Figure 1C). Pico- and nano-plankton contributed to C_f in different proportions with latitude and depth. Overall, *Prochlorococcus* spp. and nanoeukaryotes contributed most to C_f (median contribution of 55% and 25%, respectively; Supplementary Table 1). The overall median relative uncertainty of the C_f estimates was 18% and ranged from 12 to 38%.

[10] For most phytoplankton groups, the relative uncertainties in C_f were similar across provinces. However, the contributions of the uncertainties in N, ε, and D to the uncertainty in C_f were different and varied with phytoplankton group (Supplementary Table 2). For the nanoeukaryotes, most of the uncertainty was related to the uncertainty in diameter, whereas, for picoeukaryotes, the uncertainty related to the carbon-to-volume conversion factor (ε) was more important. For *Prochlorococcus* spp. and *Synechococcus* spp., the uncertainties in diameter and ε had similar weights.

[11] A significant correlation was found between $b_{bp}(470)$ and C_f (Figures 1D and 2), within $1.5Z_{eu}$. Type II regression provided the following relationship for $b_{bp}(470) < 0.003\ m^{-1}$ (or TChl-a ~ $<0.4\ mg\ m^{-3}$):

$$C_m = (30100 \pm 1100) \times \left[b_{bp}(470) - (76 \pm 4) \times 10^{-5}\right], \quad (2)$$
$$N = 229, r^2 = 0.87$$

where the uncertainties are standard deviations. We limited the use of equation (2) to $b_{bp}(470) < 0.003\ m^{-1}$ because the samples beyond that boundary value (N = 8) showed a shift in the relationship (see Discussion). The RMSD for equation (2) was 5 mgC m^{-3}, bias was 2%, and precision was 47%.

[12] We also derived a $b_{bp}(470)$-C_f relationship applicable to remote sensing algorithms, by using the subset of data from the first optical depth:

$$C_m = (27700 \pm 2000) \times \left[b_{bp}(470) - (67 \pm 9) \times 10^{-5}\right], \quad (3)$$
$$N = 70, r^2 = 0.89$$

[13] A general linear model test revealed that the regression coefficients of equation (2) (slope and intercept) were not significantly different ($p > 0.5$) from those of equation (3). RMSD for equation (3) was 4 mgC m^{-3}, bias was −5%, and dispersion was 36.1%.

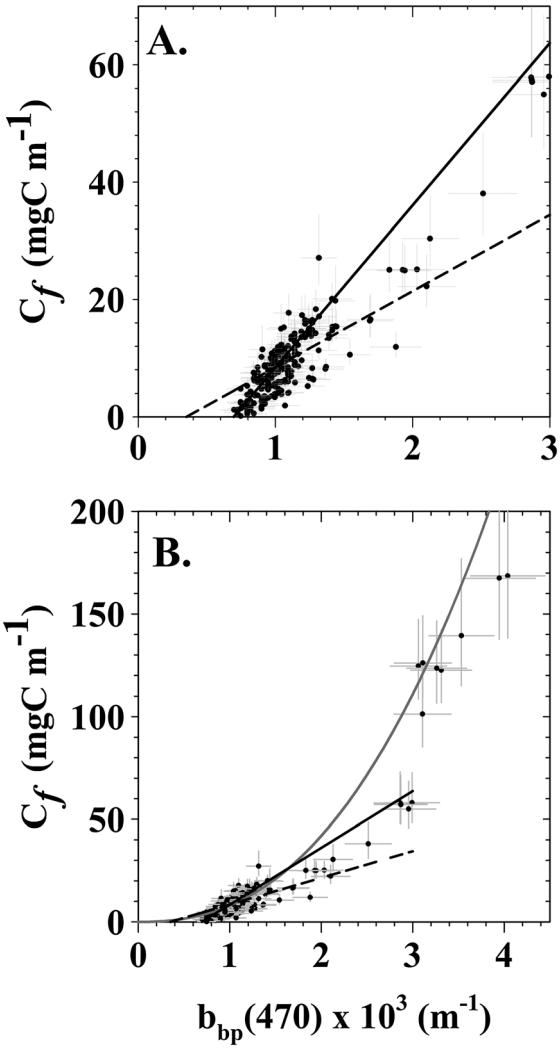

Figure 2. (A) Relationship between $b_{bp}(470)$ (see Methods for error bar definition) and C_f (filled circles, median from Monte Carlo realizations; error bar extends from the 16th to the 84th percentiles) for $b_{bp}(470) < 0.003\ m^{-1}$. (B) Relationships between $b_{bp}(470)$ and C_f for all measurements available. Black solid line: equation (3). Black dashed line: predicted C_m using *Behrenfeld et al*. [2005] model. Dark grey solid line: fit through the dataset including $b_{bp}(470) > 0.003\ m^{-1}$, corresponding to $\log_{10}(C_f) = 2.4 \times \log_{10}(b_{bp}(470)) + 8.1$, N = 237, $r^2 = 0.7$ (in log-log scale, non-error weighted regression).

[14] The model proposed by *Behrenfeld et al*. [2005] is also shown in Figure 2. Both the slope and the intercept with the x-axis ("background b_{bp}") of equation (3) were approximately double than those reported in *Behrenfeld et al*. [2005]. When compared to our dataset (N = 229), this model had a RMSD of 5 mgC m^{-3}, +7% bias, and 69% dispersion.

[15] We chose equation (3), derived from near-surface data, to illustrate the latitudinal changes in surface phytoplankton carbon at 1 h resolution (Figure 3A). The corresponding C_m:POC predictions (30 ± 20%, median ± half the central 68th percentile, N = 61) broadly agreed with the *in situ* C_f:POC estimates (40 ± 10%), and showed large latitudinal variability (Figure 3B). These ranges compared well with other *in situ* estimates of phytoplankton carbon-to-POC in the Atlantic [*DuRand et al*., 2001].

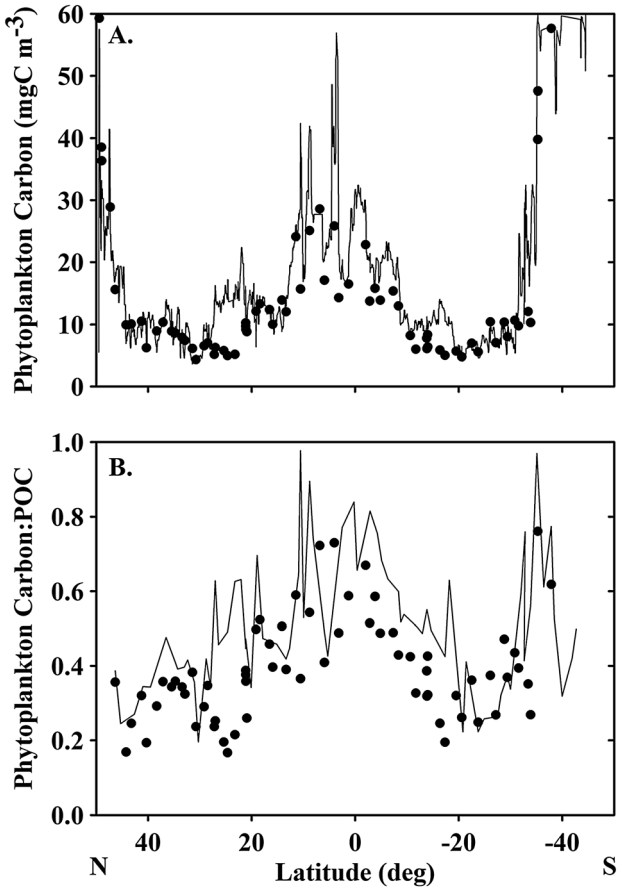

Figure 3. Latitudinal surface variations of phytoplankton carbon concentration and phytoplankton carbon-to-POC. (A) solid circles, C_f; solid line, C_m. (B) solid circles, C_f:POC; solid line, C_m:POC.

4. Discussion and Conclusions

[16] The main purpose of this study was to search for an empirical relationship between phytoplankton carbon and $b_{bp}(470)$. Although this connection has been previously suggested [*Behrenfeld et al*., 2005], it has not been tested at the scale of an ocean basin with *in situ* data. We found a significant linear relationship between $b_{bp}(470)$ and phytoplankton carbon estimated from flow cytometry (C_f).

[17] Particulate backscattering in the water column is generated by both phytoplankton and non-algal particles (i.e., bacteria, detritus, and minerals). The observed relationship between C_f and $b_{bp}(470)$ therefore implies that either phytoplankton is the dominant source of b_{bp} or that most non-algal particles covary with phytoplankton in our surface dataset. Furthermore, the intercept of equations (2) and (3) suggests the existence of another source of backscattering, which is relatively constant and independent of phytoplankton. This source may have either a natural origin (i.e., non-algal particles [*Behrenfeld et al*., 2005]) or could result from systematic uncertainties in C_f and/or b_{bp} [*Dall'Olmo et al*., 2012].

[18] The uncertainty in C_f was dominated by the contributions of its most important components: nanoeukaryotes and *Prochlorococcus* spp. The uncertainty in the cell size, and to a lesser extent, uncertainties in the C-to-volume ratio accounted for the larger part of the uncertainty in C_f. Our choice of parameters has been dictated by the desire of using the most up-to-date results for picoplankton [e.g., *Heldal et al*., 2003], while being consistent with previous AMT work. Nonetheless, we acknowledge that the characterization of these parameters (ε and D) is subject to research [*Montagnes et al*., 1994; *Menden-Deuer and Lessard*, 2000]. An alternative way to reduce the uncertainty in C_f could be by calibrating the flow cytometry measurements to estimate directly C_f, as in *DuRand et al*. [2002].

[19] Our data showed that the b_{bp}:C_f ratio was lower in eutrophic (i.e., $b_{bp}(470) > 0.003\ m^{-1}$) than in oligotrophic regions (Figure 2B). Concurrently, the fractional C_f contribution of pico- and nano-eukaryotes increased, and that of *Prochlorococcus* spp. decreased from the regions with $b_{bp}(470) < 0.0015\ m^{-1}$ to $b_{bp}(470) > 0.003\ m^{-1}$ (Supplementary Figure 1). Inclusion of C_f due to microphytoplankton (missed by flow cytometry) is expected to further decrease the b_{bp}:C_f ratio. Although only eight points are present for $b_{bp} > 0.003\ m^{-1}$, our observations are qualitatively consistent with optical theory that predicts a decrease in the b_{bp}:volume ratio with an increase in particle size (where volume is a proxy to C_f [*Boss et al*., 2004]). However, opposite predictions are obtained by using experimentally determined backscattering efficiencies [*Martinez-Vicente et al*., 2012]. Clearly, a single linear function may be insufficient to describe the relationship between b_{bp} and C_f over the entire oceanic range, and more work is needed to characterize b_{bp} and C_f in eutrophic waters dominated by large cells.

[20] We have also found that the parameters of our equation (3) are approximately double than those reported by *Behrenfeld et al*. [2005]. It is unlikely that the change in wavelength between studies (470 vs 440 nm) could account for such discrepancy: by assuming a backscattering spectral slope of −1 [*Morel and Maritorena*, 2001], we expect parameter differences of ~6%. A more plausible explanation could be that the variation in model coefficients is due to uncertainties in satellite and *in situ* estimates of b_{bp} and/or differences in the spatio-temporal scales of the two studies. An extension of this work would be to compare backscattering-based models with Chl-a-based models of C_m [*Sathyendranath et al*., 2009].

[21] Finally, we found that a smaller fraction of the POC was accounted for by phytoplankton in oligotrophic than in productive regions (Figure 3B). This result is consistent with the study of *Grob et al*. [2007] in the South Pacific, and we hypothesize that it is related to a change from a microbially dominated community (oligotrophic) to one dominated by primary producers (eutrophic).

[22] The ability to derive C_f from $b_{bp}(470)$, for $b_{bp}(470)$ values below $0.003\ m^{-1}$, means that estimates of pico- and nano-phytoplankton carbon biomass could be obtained from ocean-color satellites and *in situ* autonomous platforms. Although the range of validity of the proposed bio-optical model encompasses most of the open ocean, the regional and temporal variations of the coefficients need to be verified.

[23] **Acknowledgments.** The authors thank the captain, officers, and crew aboard RRS James Cook for their help during the AMT cruise. C. Gallienne is thanked for his help in deploying the optical package. This study was supported by the UK NERC through the UK marine research institutes' strategic research program Oceans 2025 awarded to PML and NOC, Southampton. This is contribution number 216 of the AMT programme. V.M.V. acknowledges the support of Royal Society ITG102226. Collection of optical measurements was funded by NASA grant NNX09AK30G to G.D.O. G.D.O. acknowledges support from UK NCEO and Marie Curie FP7-PIRG08-GA-2010-276812. Part of Figure 1 was made using ODV [*Schlitzer*, 2010]. Comments from T. Platt are gratefully acknowledged. We acknowledge H. Sosik and an unknown reviewer for their comments.

References

Balch, W. M., et al. (2010), Biominerals and the vertical flux of particulate organic carbon from the surface ocean, *Geophys. Res. Lett.*, *37*, L22605, doi:10.1029/2010GL044640.

Behrenfeld, M. J., and E. Boss (2006), Beam attenuation and chlorophyll concentration as alternative optical indices of phytoplankton biomass, *J. Mar. Res.*, *64*, 431–451.

Behrenfeld, M. J., et al. (2005), Carbon-based ocean productivity and phytoplankton physiology from space, *Glob. Biogeochem. Cycle*, *19*, GB1006, doi:10.1029/2004GB002299.

Booth, B. C., (1988), Size classes and major taxonomic groups of phytoplankton at two locations in the subartic Pacigic Ocean in May and August, 1984, *Mar. Biol.*, *97*, 275–286.

Boss, E., et al. (2004), Why should we measure the optical backscattering coefficient, *Oceanography*, *17*, 44–49.

Boss, E., et al. (2008), Observations of pigment and particle distributions in the western North Atlantic from an autonomous float and ocean color satellite, *Limnol. Oceanogr.*, *53*, 2112–2122.

Claustre, H., et al. (2008), Gross community production and metabolic balance in teh South Pacific Gyre, using non intrusive bio-optical method, *Biogeosciences*, *5*, 463–474.

Dall'Olmo, G., et al. (2012), Particulate optical scattering coefficients along an Atlantic Meridional Transect, *Opt. Express*, *20*, 21532–21551.

Dall'Olmo, G., et al. (2009), Significant contribution of large particles to optical backscattering in the open ocean, *Biogeosciences*, *6*, 947–967.

DuRand, M. D., et al. (2002), Diel variations in optical properties of *Micromonas Pulsilla* (prasinophyceae), *J. Phycol.*, *38*, 1132–1142.

DuRand, M. D., et al. (2001), Phytoplankton population dynamics at the Bermuda Atlantic Time-series station in the Sargasso Sea, *Deep Sea Res. Pt. II*, *48*, 1983–2003.

Gauch, H. G., et al. (2003), Model evaluation by comparison of model-based predictions and measured values, *Agron. J.*, *95*, 1442–1446.

Gordon, H. R., and W. R. McCluney (1975), Estimation of depth of sunlight penetration in sea for remote sensing, *Appl. Opt.*, *14*, 413–416.

Grob, C., et al. (2007), Contribution of picoplankton to the total particulate organic carbon concentration in the eastern South Pacific, *Biogeosciences*, *4*, 837–852.

Heldal, M., et al. (2003), Elemental composition of single cells of various strains of marine *Prochlorochoccus* and *Synechococcus* using X-ray microanalysis, *Limnol. Oceanogr.*, *48*, 1732–1743.

Holligan, P. M., et al. (1984), Vertical distribution and partitioning of organic carbon in mixed, frontal and stratified waters of the English Channel, *Mar. Ecol. Prog. Ser.*, *14*, 111–127.

Lee, Z. P., et al. (2002), Deriving inherent optical properties from water color: a multiband quasi-analytical algorithm for optically deep waters, *Appl. Opt.*, *41*, 5755–5772.

Maranon, E., et al. (2000), Basin-scale variability in phytoplankton biomass, production and growth in the Atlantic Ocean, *Deep Sea Res. Pt. I*, *47*, 825–857.

Martinez-Vicente, V., et al. (2012), Contributions of phytoplankton and bacteria to the optical backscattering coefficient over the Mid-Atlantic Ridge, *Mar. Ecol. Prog. Ser.*, *445*, 37–51, doi:10.3354/meps09388.

Menden-Deuer, S., and E. J. Lessard (2000), Carbon to volume relationships for dinoflagellates, diatoms, and other protist plankton, *Limnol. Oceanogr.*, *45*, 569–579.

Montagnes, D. J. S., et al. (1994), Estimating carbon, nitrogen, protein, and chlorophyll *a* from volume in marine phytoplankton, *Limnol. Oceanogr.*, *39*, 1044–1060

Morel, A., and S. Maritorena (2001), Bio-optical properties of oceanic waters: A reappraisal, *J. Geophys. Res. C: Oceans*, *106*, 7163–7180.

Mullin, M. M., et al. (1966), Relationship between carbon content, cell volume and area in phytoplankton, *Limnol. Oceanogr.*, *11*, 307–311.

Perez, V., et al. (2006), Vertical distribution of phytoplankton biomass, production and growth in the Atlantic subtropical gyres, *Deep Sea Res. Pt. I*, *53*, 1616–1634.

Pineiro, G., et al. (2008), How to evaluate models: Observed vs. predicted or predicted vs. observed?, *Ecol. Model.*, *216*, 316–322.

Poulton, A. J., et al. (2006a), Phytoplankton carbon fixation, chlorophyll-biomass and diagnostic pigments in the Atlantic Ocean, *Deep Sea Res. Pt. II*, *53*, 1593–1610, 10.1016/j.dsr2.2006.05.007.

Poulton, A. J., et al. (2006b), Phytoplankton mineralization in the tropical and subtropical Atlantic Ocean, *Glob. Biogeochem. Cycle*, *20*, 10, Gb4002. doi:10.1029/2006gb002712.

Sathyendranath, S., et al. (2009), Carbon-to-chlorophyll ration and growth rate of phytoplankton in the sea, *Mar. Ecol. Prog. Ser.*, *383*, 73–84.

Saunders, R. (1991), Comparative study of the biochemical composition of selected species of phytoplankton in the Plymouth Culture Collection, in *Undergraduate dissertation*, edited, Plymouth Marine Laboratory, Plymouth, UK.

Schlitzer, R. (2010), Ocean Data View, http://odv.awi.de.

Stramski, D., et al. (2008), Relationships between the surface concentration of particulate organic carbon and optical properties in the eastern South Pacific and eastern Atlantic Oceans, *Biogeosciences*, *5*, 171–201.

Strathmann, R. R. (1967), Estimating the organic carbon content of phytoplankton from cell volume or plasma volume, *Limnol. Oceanogr.*, *12*, 411–418.

Tarran, G. A., et al. (2006), Latitudinal changes in the standing stocks of nano- and picoeukariotic phytoplankton in the Atlantic Ocean, *Deep Sea Res. Pt. II*, *53*, 1516–1529.

Tarran, G. A., et al. (2001), Microbial comunity structure and standing stocks in the NE Atlantic in June and July of 1996, *Deep Sea Res. Pt. II*, *48*, 963–985.

Van Heukelem, L., and C. S. Thomas (2001), Computer-assisted high-performance liquid chromatography method development with applications to the isolation and analysis of phytoplankton pigments, *J. Chromatogr. A*, *31–49*.

Zubkov, M. V., et al. (2000), Picoplankton community structure in the Atlantic Meridional Transect: A comparison between seasons, *Progr. Oceanogr.*, *45*, 369–386.

Zubkov, M. V., et al. (1998), Picoplanktonic community structure on an Atlantic transect from 50 N to 50 S, *Deep Sea Res. Pt. I*, *45*, 1339–1355.